Understanding the nature of massive dusty star-forming galaxies at high-z with ALMA spectral imaging.

Gayathri Gururajan, Matthieu Béthermin, Patrice Theulé, Justin Spilker and the SPT-SMG collaboration

GALAXIES FAR FAR AWAY

- Massive (> 10^{11} $M_\odot$) DSFGs with high star formation rate (500 - 3000 $M_\odot$ /yr) can be found in the high-redshift universe.
- These galaxies could also be the progenitors to Central cluster galaxies seen today (Lilly+99, Swinbank+06, Hickox+12).
- What drives the intense star formation?
- Characterising the gas reservoir —> Nature of these monsters

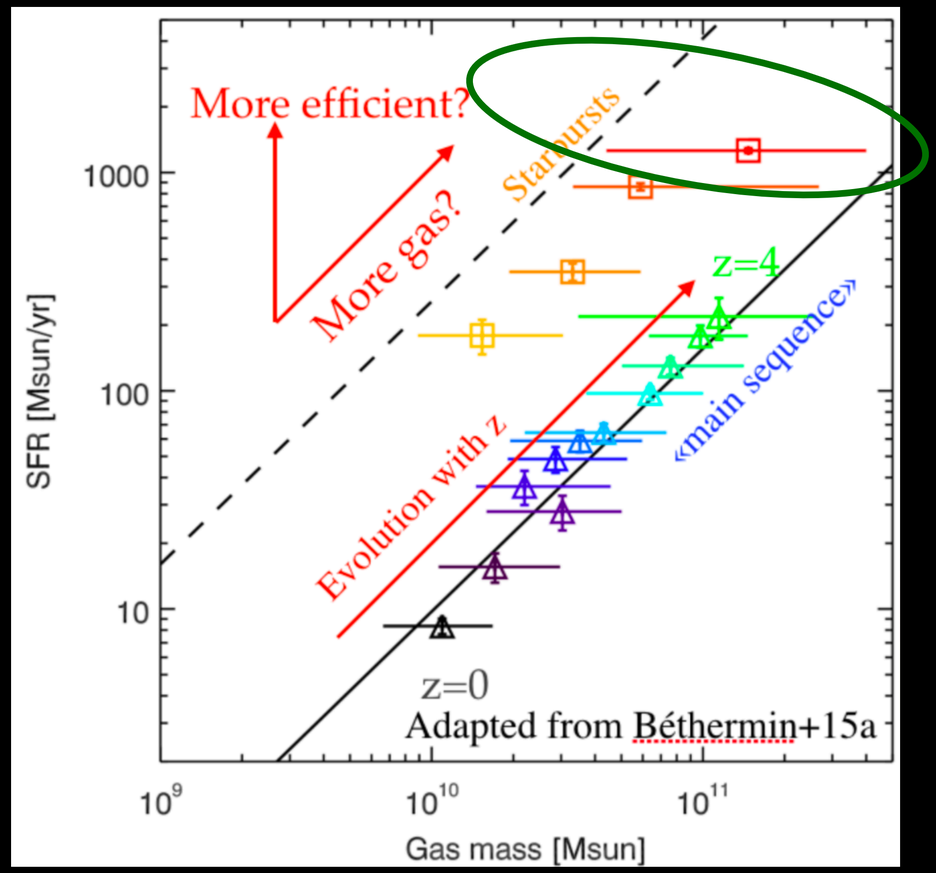

Estimating the gas content

- Traditionally gas mass tracer - CO(1-0)
- Alternatively tracer - [CI] lines
- High-J CO lines —> warm and dense molecular gas
- The total dust continuum —> IR luminosity.
- Gravitationally lensed sample —> Better resolution, shorter time

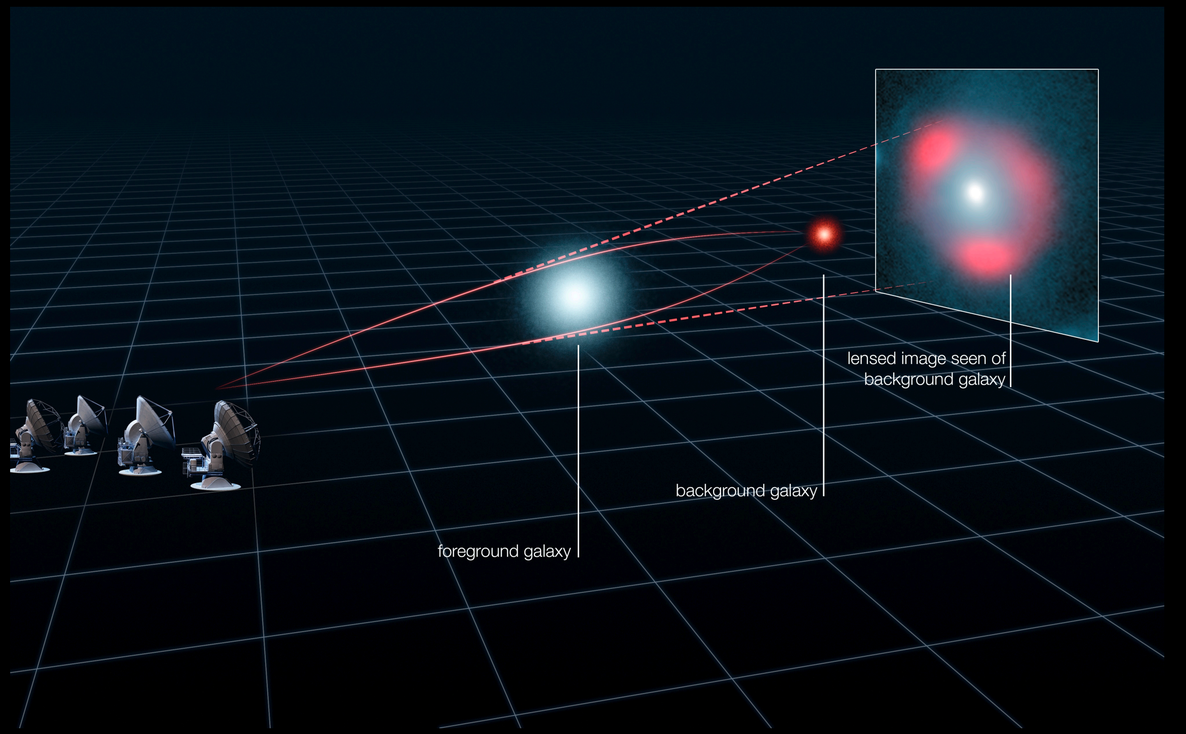

Building a statistical sample of [CI] observations of lensed DSFGs at z~2-4 with ALMA-ACA

Sample

- Target : SPT sources with both [CI] transitions in the observation window (30 galaxies).
- Ancillary low-J CO data and dust mass estimations
- This sample therefore gives us the unique ability to understand the properties of [CI] lines.
- Aim : To compare the ability of [CI], CO and dust as tracers of gas mass.

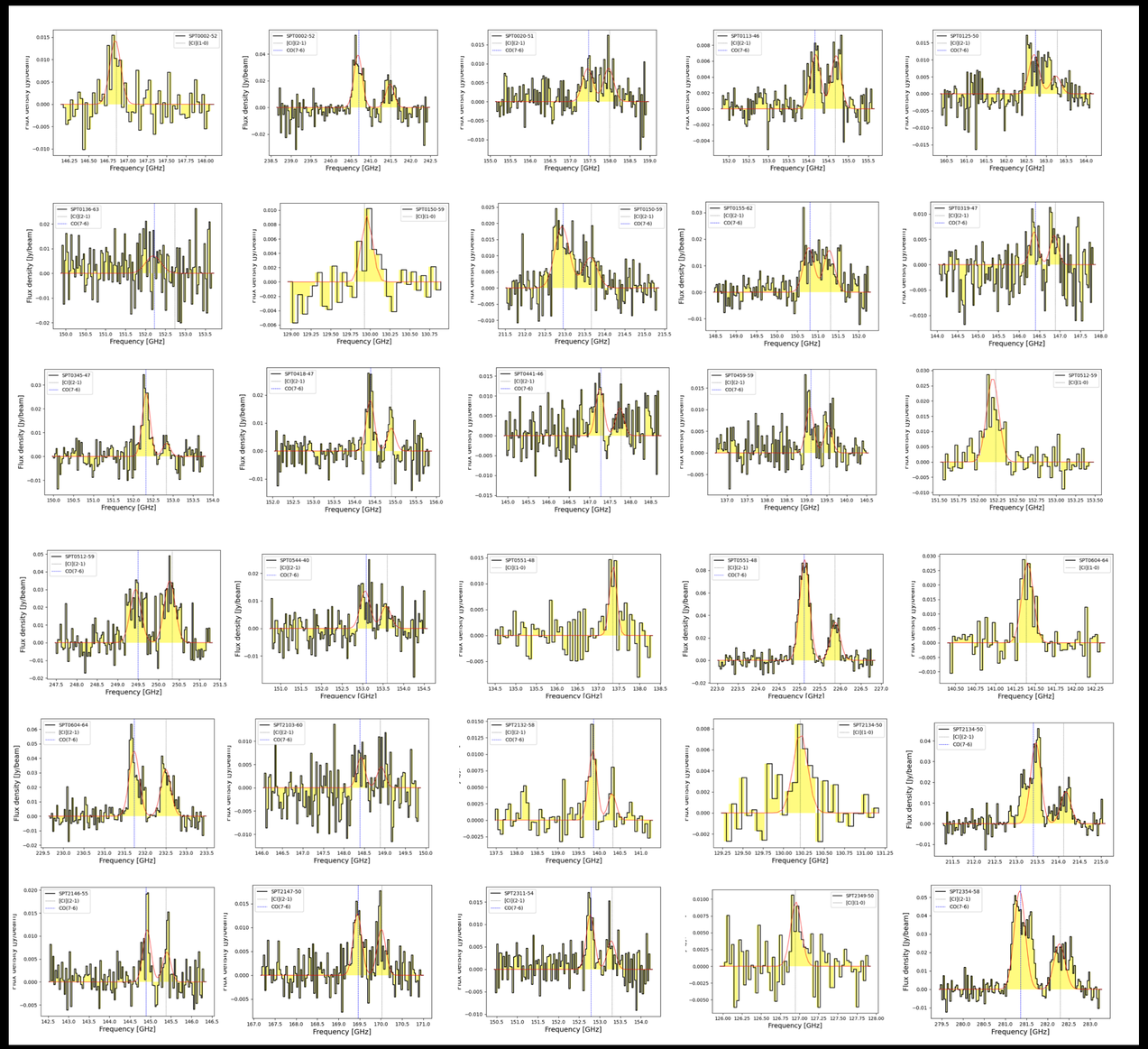

Gururajan+ in prep.

[CI] excitation and dust temperature

- We compute the [CI] excitation temperature with $L'_{[CI](1-0)}$ and $L'_{[CI](2-1)}$.
- Most of our sources have larger dust temperature than the [CI]-excitation temperature.
- Pausible explanation : The dusty cores of these galaxies are warmed by the intense star formation, whereas the [CI] is present in more extended regions.

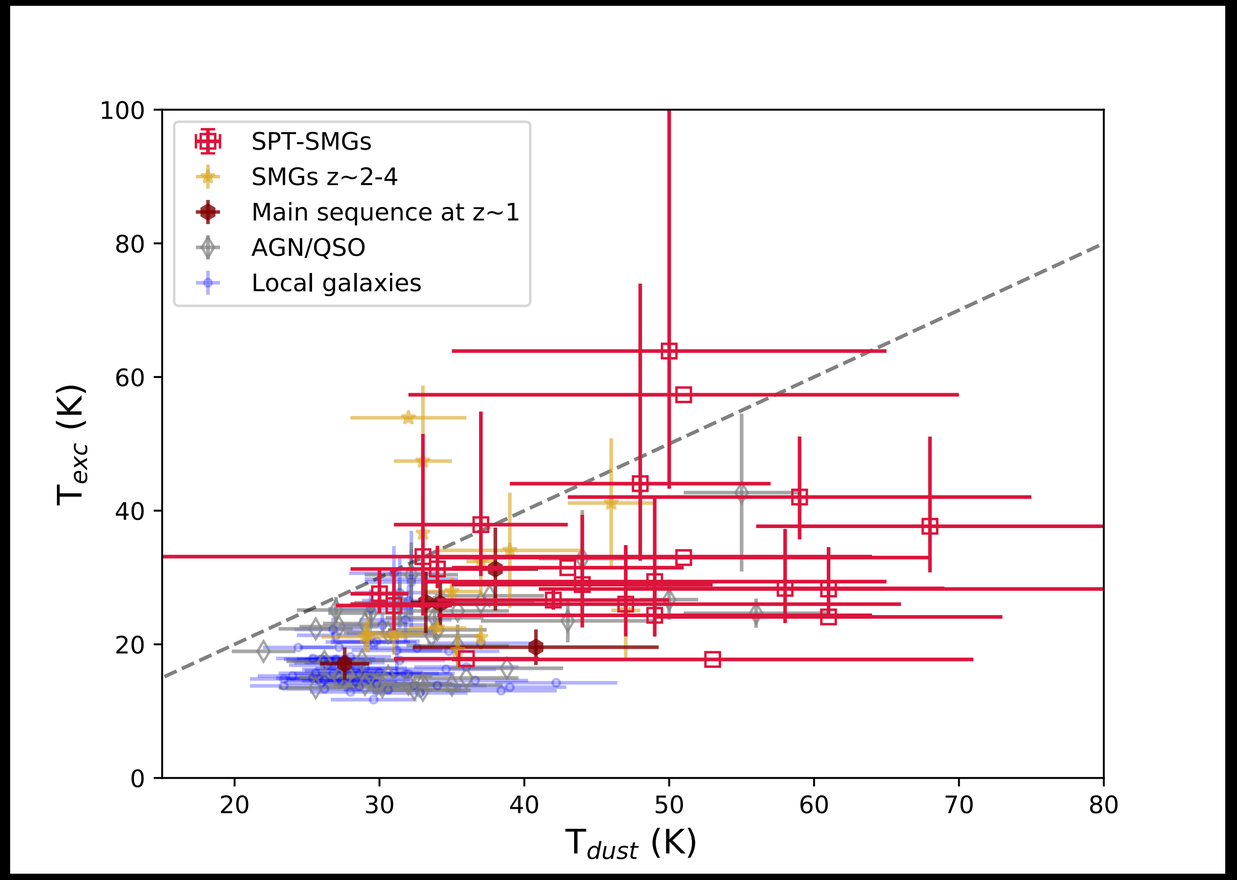

Gururajan+ in prep.

Gas mass traced by CO, [CI] and dust

- We compute the gas mass estimated by [CI](1-0), low-J CO lines and the dust mass.
- For [CI] estimated mass, the uncertainty can mainly arise from the assumed XCI factor.
- In the case of CO-derived gas masses, the assumed alphaCO is highly debated.
- We try to use the gas mass estimated by these tracers to cross-calibrate the XCI, alphaCO and GDR.

$$M_{H_2}^{CO} = M_{H_2}^{dust}$$

$$\frac{L'_{CO}}{M_{dust}} = \frac{\delta_{GDR}}{\alpha_{CO}}$$

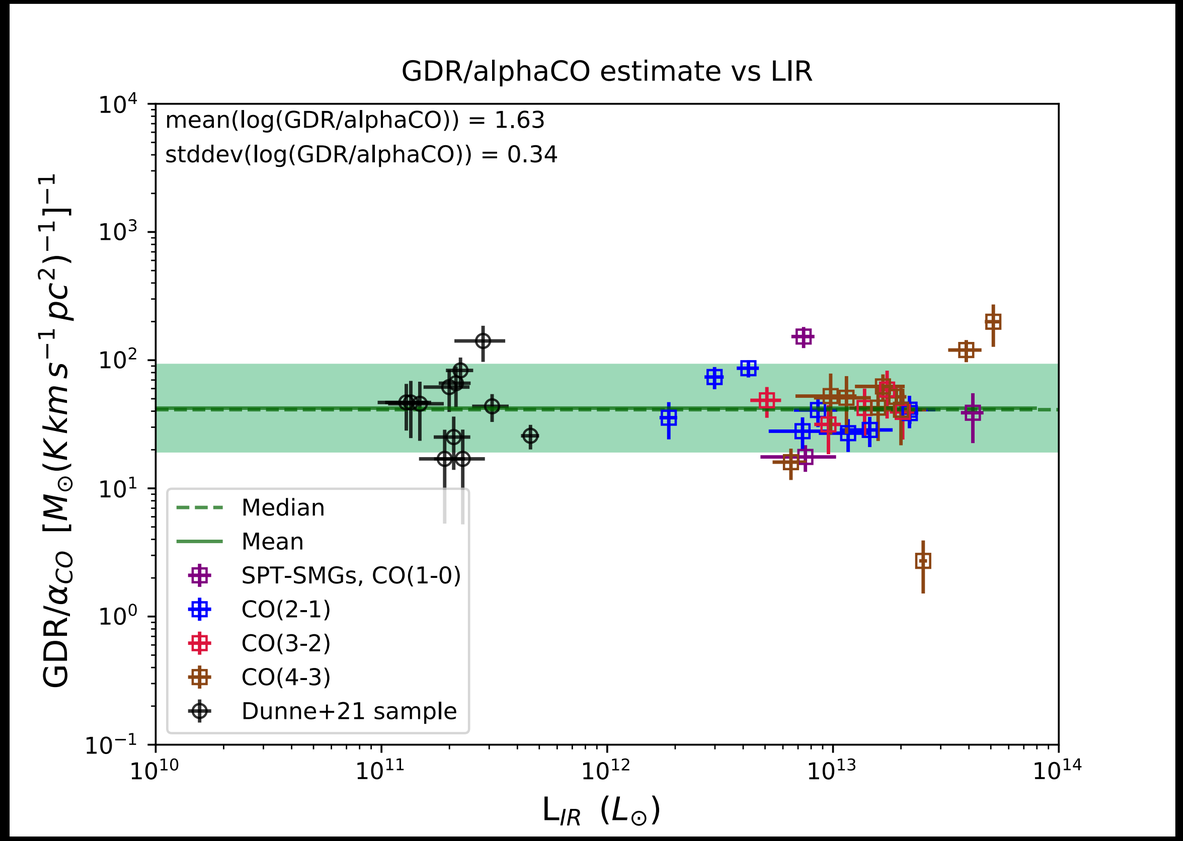

Gururajan+ in prep.

High resolution spectral imaging of CO(7-6), [CI](2-1) and dust continuum of 3 high-z lensed DSFGs with ALMA.

Gururajan+22

Sample

- Our sample - SPT0103-45 (aka, Ia precious), SPT2147-50 and SPT2357-51 from the SPT sample (Vieira+13, Strandet+16, Aravena+16, Spilker+16, Reuter+20).

- [CI](2-1), CO(7-6) and dust continuum observed with ALMA band 5 at a resolution of 0.3 arcsec and S/N > 14.

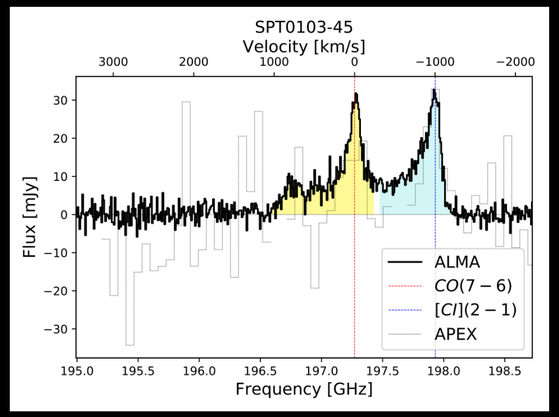

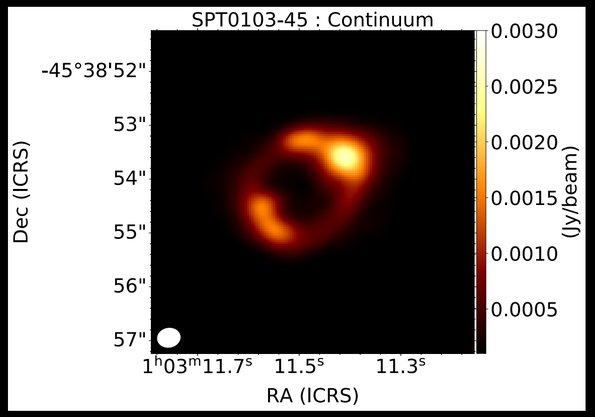

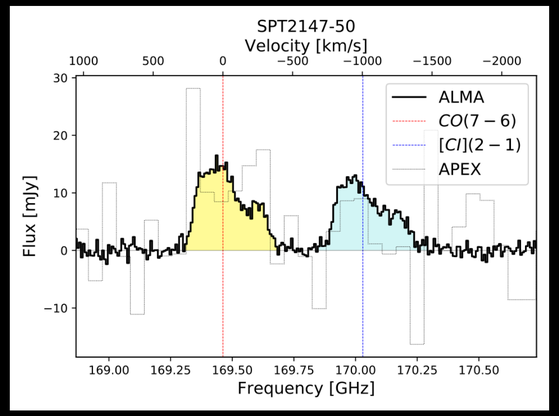

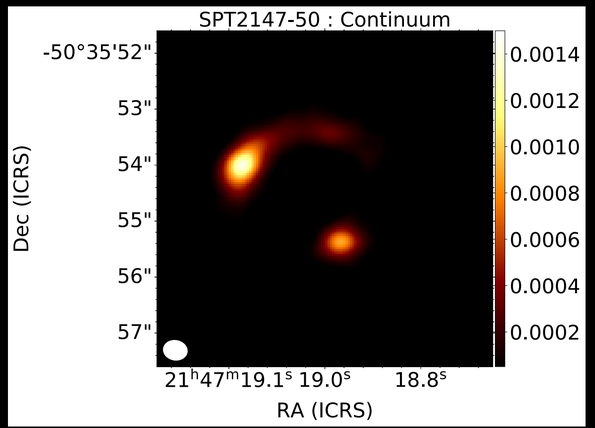

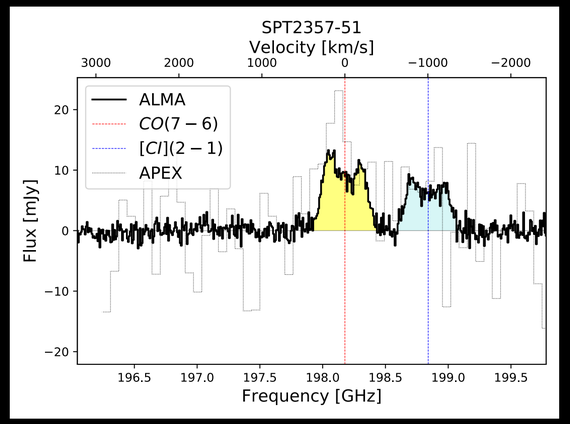

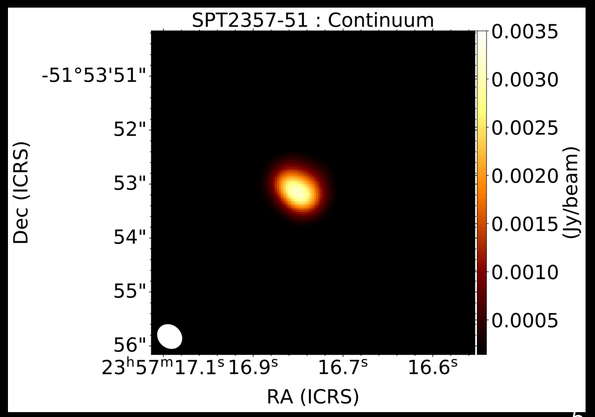

Image-plane kinematics

- For SPT0103-45 and SPT2147-51, we construct pixel-wise velocity maps for both the line emissions.
- The velocity maps of both the sources show a smooth gradient which could be suggestive of their rotation.
- SPT2357-51 shows a double peak profile for both the lines in its integrated spectra. We use a 2-component gaussian decomposition for both these lines.
- The blue component (low-velocity component) shows a smooth gradient for both the lines, where as the gradient in the red component (high-velocity) is disturbed.

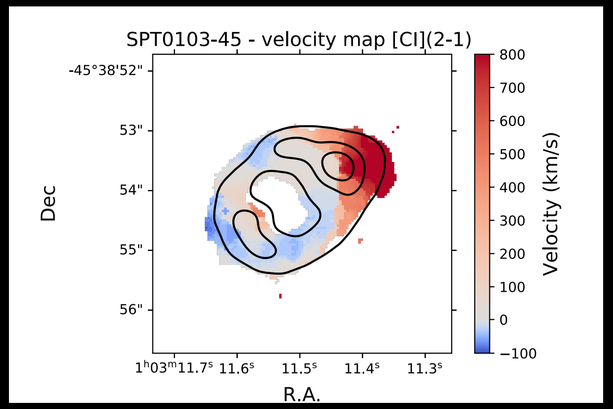

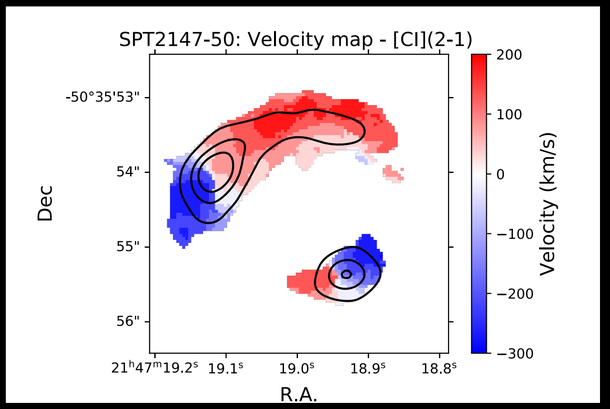

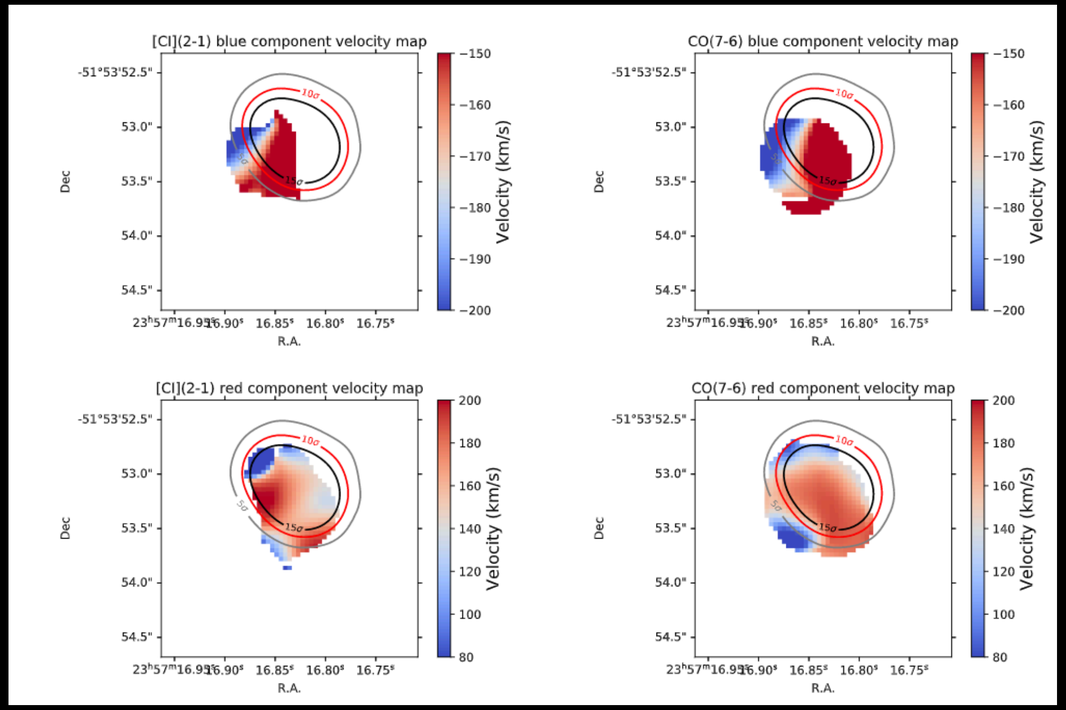

Reconstructed source-plane velocity maps

- To model the source-plane velocity, we plot the positions from the lens modeling of the line emissions for every velocity bin.
- For SPT0103-45 and SPT2147-50, we can see a smooth gradient in the positions with the velocities.
- This could be suggestive of the sources being rotating disks.

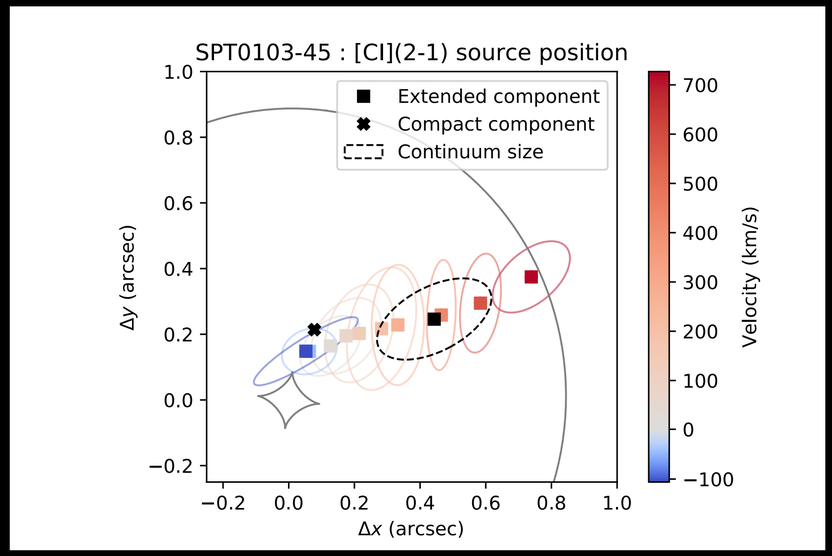

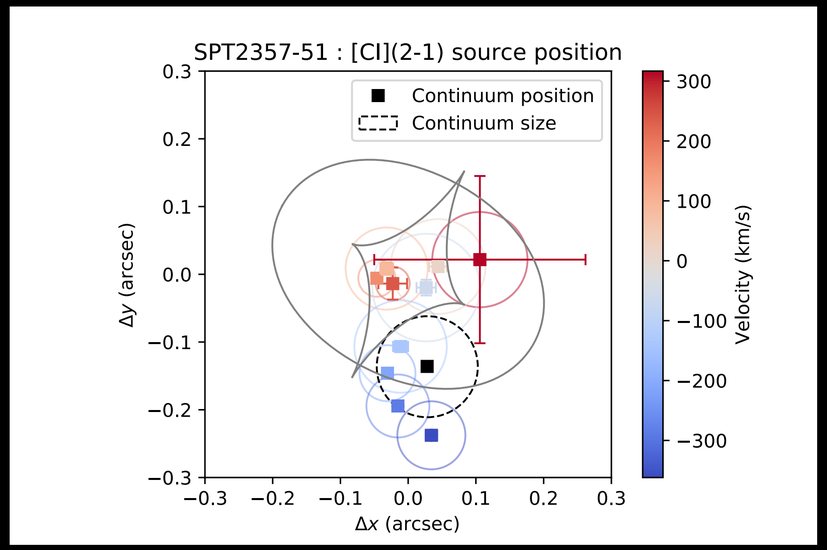

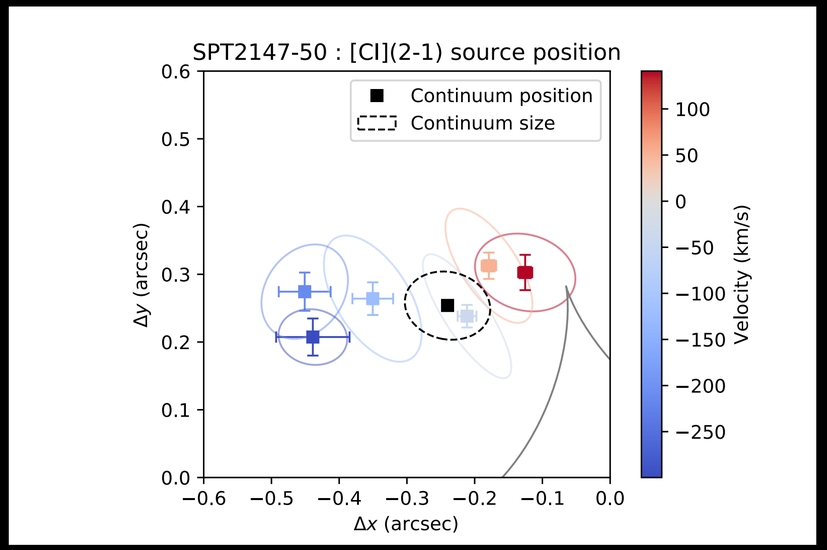

Resolved line and continuum ratios

- We computed the $L_{[CI](2-1)}/L_{CO(7-6)}$ and $L_{[CI](2-1)}/L_{IR}$ ratios of sample and compared them with other SMGs and main sequence galaxies presented in Valentino+20 compilation.

- $L_{[CI](2-1)}/L_{CO(7-6)}$ is parallel to the density iso-contours thereby being a density proxy and similarly, $L_{[CI](2-1)}/L_{IR}$ being a proxy of the radiation field.

- The ISM of our sources (pixels in the figure) exhibit a heterogeneity, showing variations in the radiation field and density across the source.

- Our sample have comparable radiation field intensities and densities to the SMGs and main sequence galaxies at z~1.

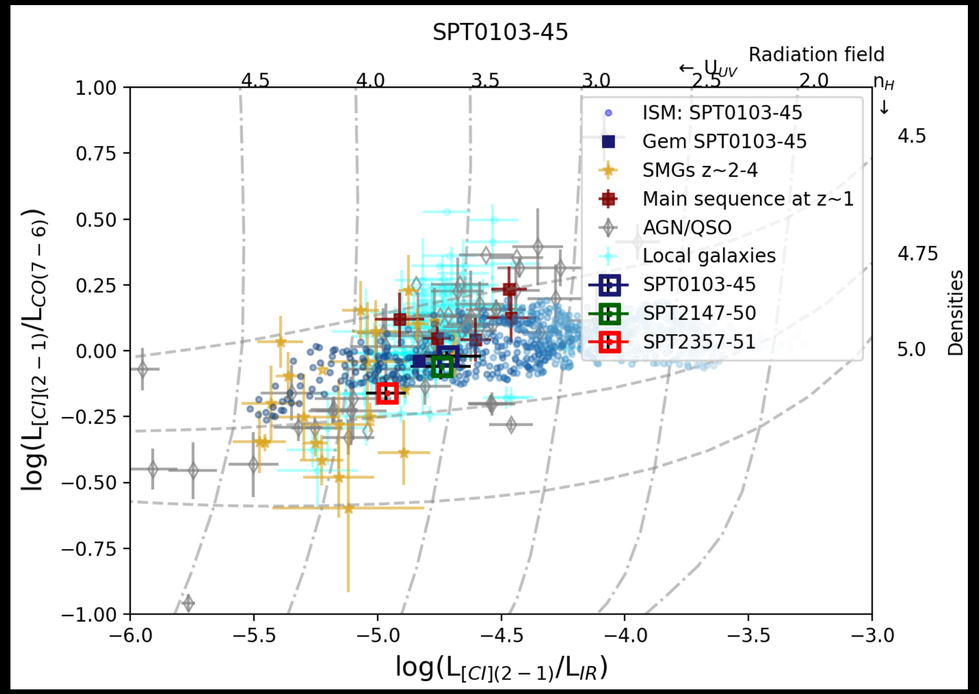

Valentino+20 sample

Walter et al. 2011; Alaghband-Zadeh et al. 2013; Bothwell et al. 2017; Yang et al. 2017; Andreani et al. 2018; Can˜ameras et al. 2018; Nesvadba et al. 2018; Dannerbauer et al. 2019; Jin et al. 2019

Results

- High intrinsic SFR > 800 $M_\odot$ / yr.
- From the source size estimates and axis ratios, we compute the Σ_{SFR} and dynamical mass using a simple Keplerian approach.
- Gas mass estimated with α_{CO} = 0.8 was agreeable with the dynamical mass, a higher α_{CO} = 3.4 gas mass was in tension with the dynamical mass.
- This gives a short depletion time scale < 100 Myr (gas mass with α_{CO} = 0.8)
- GDR estimated with α_{CO} = 0.8 was low~44, Plausible reason : High metallicity?

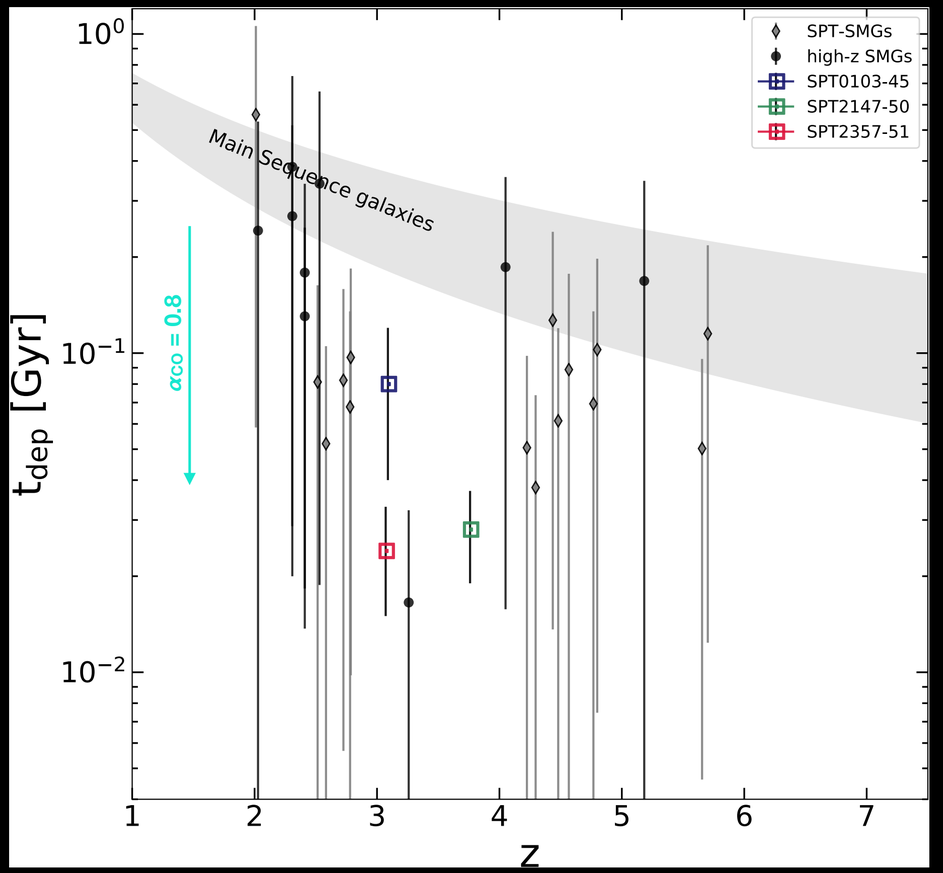

Conclusions

Large sample

- With the large sample, we compare the gas excitation to the dust temperature - No source found with very low dust temperature.
- We probe the radiation field and densities of the ISM using line ratios, our sample has comparable intensities and densities to the SMGs in literature.
- We provide cross-calibration for the uncertain parameters like α_{CO}, XCI and δGDR.

High-resolution sample

- Although the sources have agreeable radiation field and densities as the other SMGs, their ISM is heterogenous.
- Gas mass estimated with $\alpha_{CO} = 0.8$ was agreeable with the dynamical mass, a higher $\alpha_{CO} = 3.4$ gave longer depletion time scale, but the gas mass was in tension with the dynamical mass.
- We can conclude that our sample is morpho-kinematically diverse with rotating (starbursting) disks to merging systems.

Thank you for your attention!

Source	SFR	sSFR	tdep	Mgas*10^10	Mgas_CI*10^11	Mdyn*10^10
SPT0103-45	1900+/-600	69+/-20	91+/-14	17+/-3	-	16+/-4
SPT2147-50	830+/-200	30+/-7	28+/-2	2.3+/-0.1	6.8+/-0.5	2.5+/-0.4
SPT2357-51	1620+/-260	59+/-10	26+/-5	4.1+/-0.8	-	-

$$M_{dyn} = \frac{R\,V_{obs}^2}{G\sin^2(i)} \qquad (\cos i = b/a)$$

Position - velocity diagram

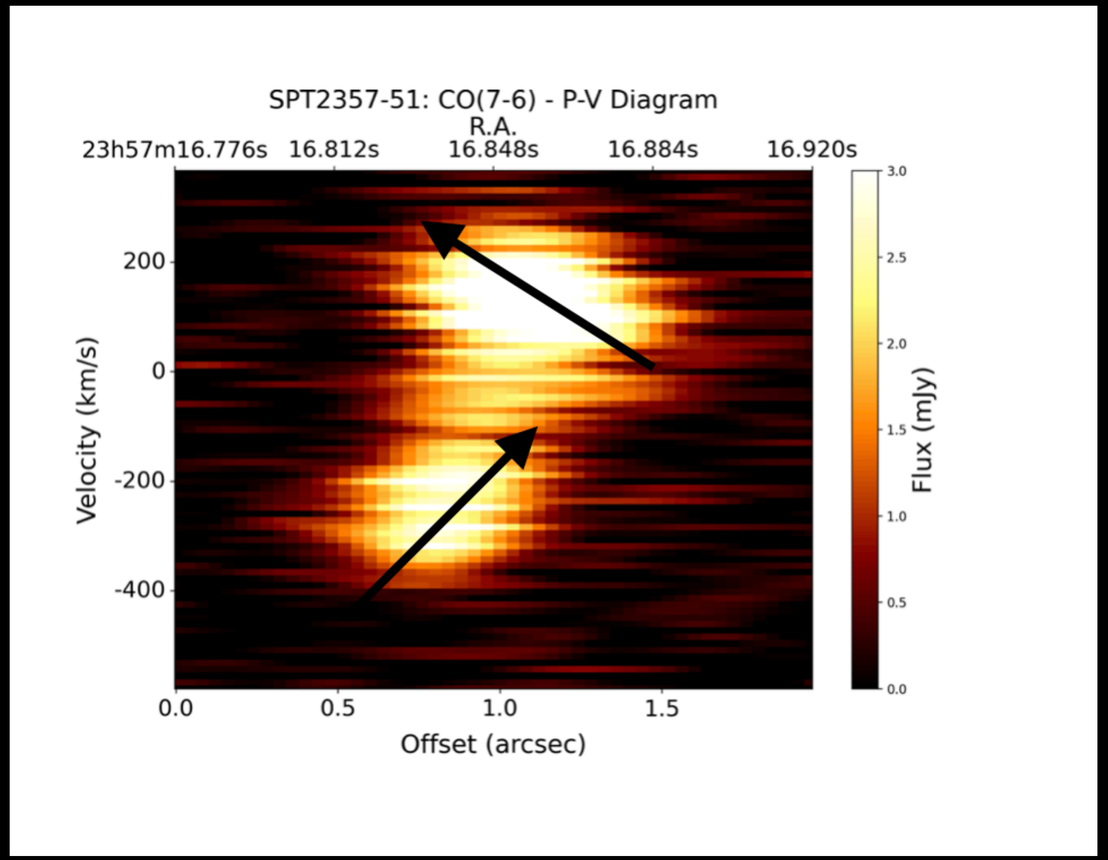

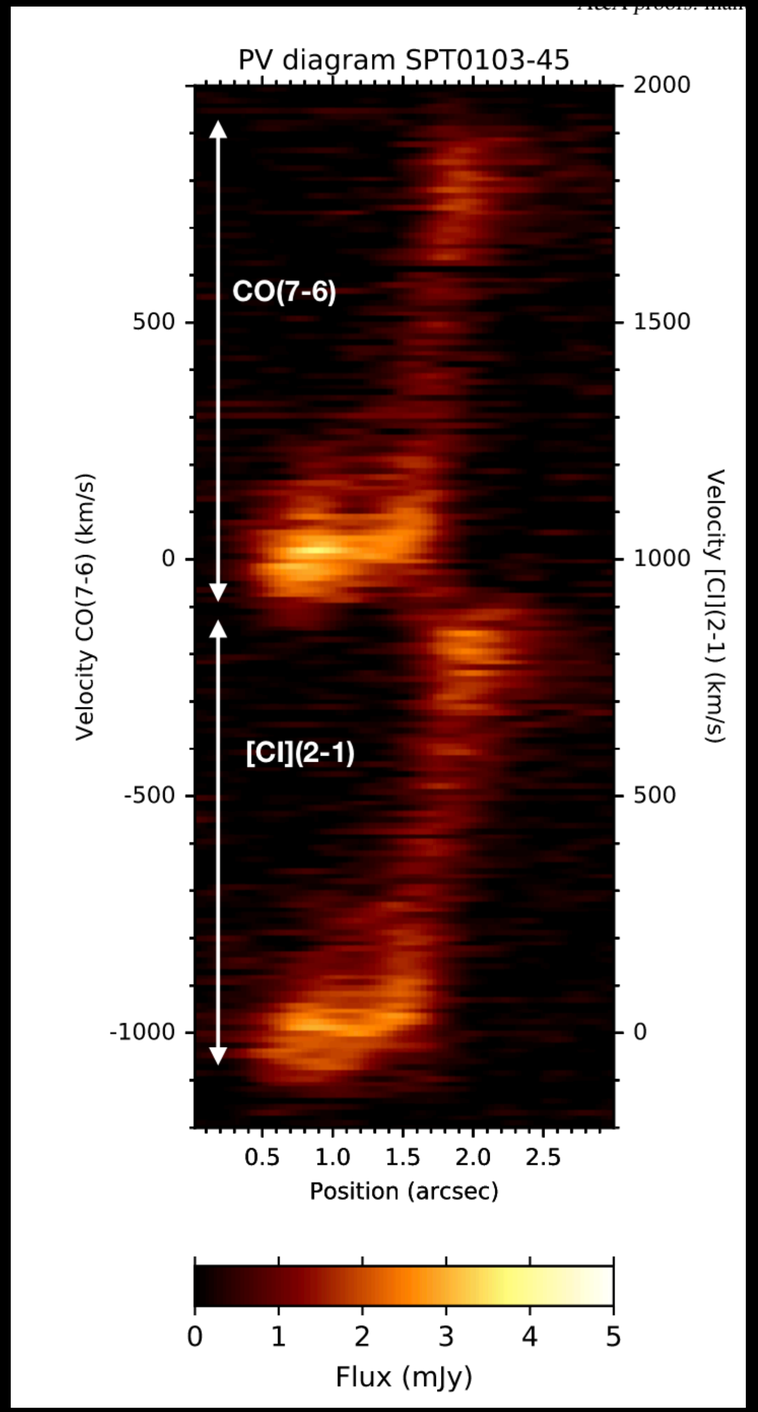

Lens modelling

- We use the visibility-based modelling code visilens (Spilker+16).
- For SPT0103-45 we model the continuum emission using a two-component source profile. For SPT2147-50, we modelled using a single Sérsic source profile and SPT2357-51 we used a single Gaussian profile.
- To model the line emissions, we divide the data into velocity bins of ~500 km/s and model each of these bins.
- Using our best fit continuum model parameters as starting values, and fixing the best fit lens parameters, we model the line emission of all our sources.

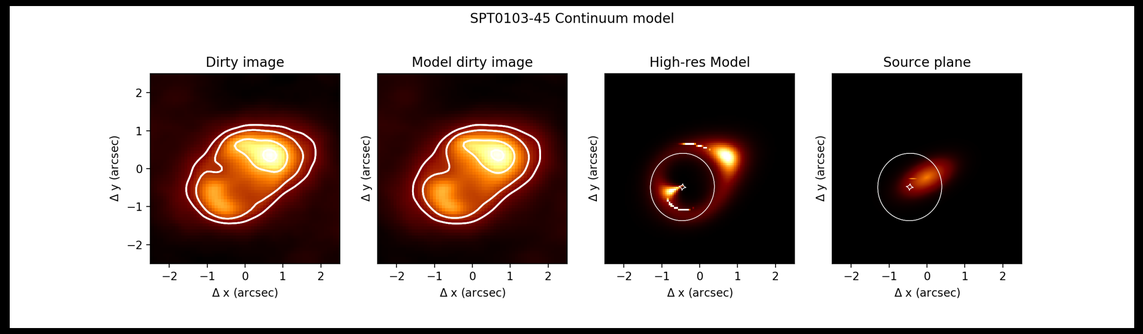

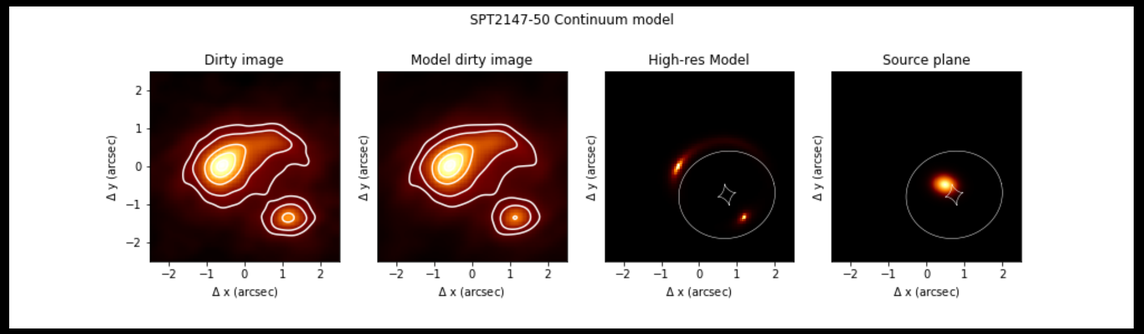

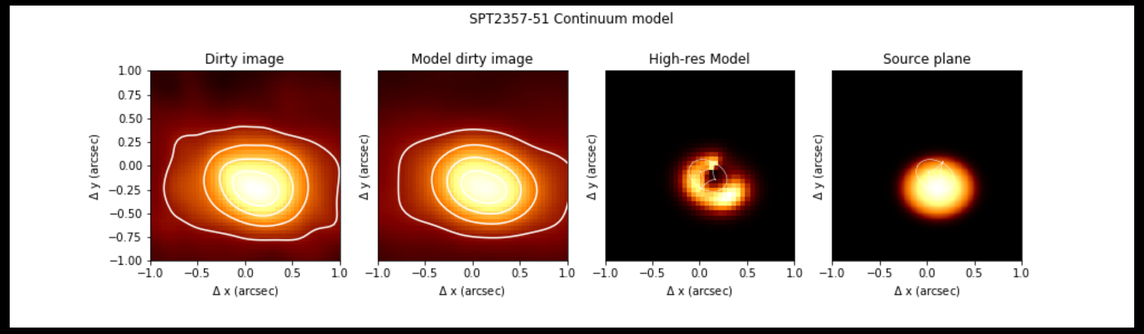

Differential magnification

- We explored possible differential magnification effects in the lines observed in our sources comparing the effective magnification of the lines to the continuum magnification.
- The variations were < 24% for our sources hence there was no significant difference in the line fluxes.
- However, the asymmetries observed in the line profiles of SPT0103-45 and SPT2147-50 arise due to magnification effects.
- The plot shows the magnification as a function of velocity for the [CI](2-1) and CO(7-6) lines compared to the observed line profiles of our sources.